LITERATURE REVIEW

Aykut ER, Egeberk ÖZBERK

Computer Engineering, Çankaya University, Turkey
c1311018@student.cankaya.edu.tr
c1411045@student.cankaya.edu.tr

Abstract - With the advances in the computer world, our image processing techniques, our algorithms and our methods became much more efficient and precise. For this reason image processing is now included in almost every field of work including medical devices and their software. One of the branches where image processing meets medical computer science is the blood vessel segmentation. Segmentations with high accuracy allow a better look at the vessels of the retinal images therefore even a faster diagnosis for eye diseases such as macular degeneration or diabetic retinopathy, which is now the leading cause for blindness at mid ages [1]. The segmentation of retinal blood vessels has been a heavily researched area in recent years [2] and they achieve different results in terms of accuracy, precision and sensitivity. They consist of different algorithms, methods, techniques and some even merged different algorithms into a single hybrid method. Several studies for retinal vessel segmentation have been introduced and some of these studies are described below.

Keywords: Blood Vessel Segmentation - Texture Classification - Gabor Filter - Gabor Energy - FCM clustering - Retinal Imaging - Diabetic retinopathy - Macular degeneration - Otsu's method - Thresholding - Image Matting - Fundus Image - ACS Algorithm - Hu Moment-Invariants.

Blood Vessel Segmentation with Image Processing

1) Gabor Filter Method

In 2007, Alauddin Bhuiyan, Baikunth Nath, Joselito Chua and Ramamohanarao Kotagiri proposed a texture based vessel segmentation method to overcome the problem that is the division of the entire vessel is not easy due to the changes in the constructions in the small vessels.

The proposed method is based on blood vessel segmentation and texture classification of vessels and non-vessels in color retinal images [3]. One of the reasons for developing this method is that the texture analysis performs well in determining the vessel and non-vessel parts of the images. Another reason is that the original images are contained in RCB color pixels and the addition of color to the texture analysis due to the color distributions in the images makes the process even easier. 3D RGB space does not contain colors that people can perceive [3]. So, uniform color spaces are used along with RGB color channels to find the textures.

Due to high contrast for texture analysis, E and Eλ in the Gaussian color space, L luminance in L*a* b color space, and green channel G in RGB color space are selected. Adaptive Histogram Equalization (AHE) method [4] is applied to these four color space images. For these color channels, a Gabor filter with twenty-four directions and three wavelengths is applied to determine the textures.

After the texture clusters are analyzed and the texture image is formed, a feature vector is generated for each pixel in the texture image. These vectors are classified as a vessel or background part [3] using unsupervised FCM clustering algorithms [5-6]. The result of this algorithm is to create a 2D matrix and transform the cluster numbers to binary values to generate a segmented image. In general, the technique of method is shown in figure 1.
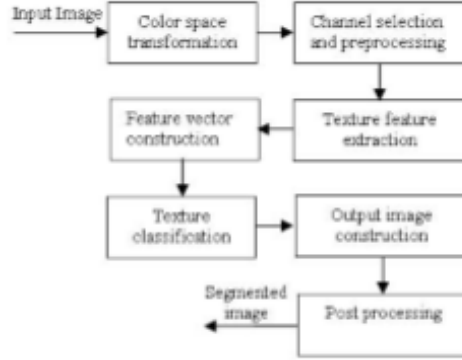

Figure 1 Vessel Segmentation Model

Generally, the image data is produced is RGB and the L*a*b* definition is based on a system known as CIE XYZ space (ITU-Rec 709) [3]. This space is produced in RGB [7] and XYZ is defined as:

$$X = 0.412453R + 0.357580G + 0.180423B$$
$$Y = 0.212671R + 0.715160G + 0.072169B$$
$$Z = 0.019334R + 0.119193G + 0.950227B$$

The L*a*b* color space is defined as follows:

$$L^* = 116f(Y/Y_n) - 16$$
$$a^* = 500[f(X/X_n) - f(Y/Y_n)]$$
$$b^* = 200[f(Y/Y_n)] - f(Z/Z_n) \tag{1}$$

Where f (q) = q1/3 if q<0.008856 otherwise f (q) = 7 .87+ 16/116. Xn, Yn and Zn represent a reference white as defined by a CIE standard illuminant [1]. This is obtained by setting R = G = B = 100 in formulas of X, Y, Z above, q ∈ {X/Xn, Y/Yn, Z/Zn} [3]. The first three components of Gaussian color model are calculated by the following formula, taking λ0 = and σλ = 55nm [8] and the Gaussian model is converted into RGB with these calculations.

$$\begin{pmatrix} \hat{E} \\ \hat{E_\lambda} \\ \hat{E_{\lambda\lambda}} \end{pmatrix} = \begin{pmatrix} -0.48 & 1.2 & 0.28 \\ 0.48 & 0-0.4 & -0.4 \\ 1.18 & -1.3 & 0 \end{pmatrix} \begin{pmatrix} X \\ Y \\ Z \end{pmatrix} \tag{2}$$

A Gabor filter has poor response on smooth surfaces in the background. In other words, when the Gabor filter changes the orientation parameter of a vessel, it makes large differences in its results [9]. This shows that the Gabor filter is a very useful solution for texture analysis. The Gabor filter based texture analysis method was applied as described below.

A Gabor filter is produced from an image I(x,y), (x,y) ∈ Ω, where Ω is the set of image points, and a Gabor function g(x,y), (x,y) ∈ ω.

$$r(x,y) = \iint\limits_{\Omega} I(\xi,\eta)g(x - \xi, y - \eta)d\xi d\eta \tag{3}$$

The following Gabor function is used to model the spatial summation properties of an image.

$$g_{\xi,\eta,\lambda,\Theta,\phi}(x,y) = \exp(-\frac{x'^2 + \gamma^2 y'^2}{2\sigma^2})\cos(2\pi\frac{x'}{\lambda} + \phi)$$
$$x' = (x - \xi)\cos\Theta - (y - \eta)\sin\Theta$$
$$y' = (x - \xi)\cos\Theta - (y - \eta)\sin\Theta \tag{4}$$

Where x and y represent a light impulse position and ξ,η,σ,γ,λ,Θ,φ parameters. (ξ, η) pair represents a center of receptive field in the image. The standard derivation in Gaussian σ, determines the size of the receptive field and eccentricity of the receptive field ellipse is determined by the parameter γ called the spatial aspect ratio. This ratio is between 0.23<γ<0.92 and this value is taken as 0.5 in this work [3]. Where λ is the wavelength of the cosine factor and spatial frequency is calculated as 1/λ. The parameter Θ specifies the orientation of the normal to the parallel excitatory and inhibitory stripe zones [3]. Also, the parameter φ ∈ (−π, π), which is a phase offset argument of the harmonic factor cos(2πx'/λ + φ) [3], is the symmetric function of the main function and The result for values of 0 and π of this parameter is symmetric according to receptive field, and the result for values of −1/2π and 1/2π of this parameter is asymmetric according to receptive field. In all other cases the result is asymmetric. In this study, φ values are 0 and 1/2π.

By combining the results obtained from the images filtered with Gabor filter, the amount of Gabor energy is calculated by following formula.

$$E_{\xi,\eta,\Theta,\lambda} = \sqrt{r^2_{\xi,\eta,\Theta,\lambda,0} + r^2_{\xi,\eta,\Theta,\lambda,\pi/2}} \tag{5}$$

The values in the square root of this formula are the results obtained from symmetric and asymmetric filters.

The maximum response value in the color channels is reduced the complexity in the training on data and the length of the feature vector. They also generate an image for histogram analysis and for each color channel to determine the cluster number. For each pixel from these images, the feature vector of length of twelve elements is classified according to vessel and non-vessel using FCM [5-6] algorithm [3].

FCM is a cluster technique, and the purpose of this algorithm is to reduce the cost function of Fuzzy-C-Means by the following formula [6].

$$J(U,V) = \sum_{j=1}^{C}\sum_{i=1}^{N}(\mu_{ij})^m\|x_i - v_j\|^2 \tag{6}$$

V is the cluster centers and U is fuzzy partition matrix [3]. The U matrix satisfies the following conditions.

$$\mu_{ij} \in [0,1], \forall i = 1,..,N, \forall j = 1,..,C$$

$$\mu_{ij} = 1, \forall i = 1,..,N \tag{7}$$

In the formula, the base value m determines the fuzziness of cluster. The most commonly used distance formula is the Euclidean distance ($d_{ij} = \|x_i - v_j\|$).

The values of this technique is calculated using the DRIVE [11] database. For performance evaluation, we detected the vessel center line in our output segmented images and hand labeled ground truth segmented (GT) images applying the morphological thinning operation. Since the vessel width in the GT images does not always coincide with the position of the vessel, the images in which the segmentation process is performed cannot be compared with the GT images. In their work, five skeletonized images are compared with GT images and they assume a maximum of two pixels in the images. In general, 84.37% sensitivity and 99.61% specificity were obtained. But they did not specify the accuracy rate in their work. So we do not know exactly about the performance of the work. According to their performance gives good results compared to other studies, like Hoover et al. [12] method.

In this method, vessel width and vessel bifurcation and crossover detection calculations are not carried out, so extra procession is performed on the images for these calculations, but those who develop this method continue to work on these problems.

2) Ant Colony System Algorithm

In 2013, another study related for vessel segmentation [13] has done Ahmed Hamza Asad, Ahmad Taher Azar, Mohamed Mostafa M. Fouad, Aboul Ella Hassanien. Their approach is mainly based on an algorithm called ant colony system and they've also used a modified version of their old heuristic function for improvement. Their proposed method consists of 4 steps:

- Preprocessing
- Features computation
- ACS based segmentation
- Post-processing

In preprocessing step, green channel of the original image is extracted since it provides the best contrast harmony between vessel and the background and because of the fact that green channel image will be used in further processing, its contrast is enhanced. After enhancements, reflection of the optic disc is removed as its overlapping with some of the central vessels' lengths.

The features computation process aims to distinguish vessels from the background by correcting varying illumination in background. Correction is achieved by computing homogenized background and gray-level based features (f_2, f_5) [13]. After obtaining gray-level based features, vessel-enhanced image is computed it's gray-level (I_{ve}) is used for used for computing Hu moment-invariants based feature (Hu_1) (detailed in [14]) as well as it's selected feature by CFS (detailed in [15]) [13].

The main method used for segment blood vessels in this approach is an improved version of ant colony system algorithm proposed by Dorigo et al. [16]. Purpose of this algorithm was solving the travelling salesman (TSP) and it's based on behavior of real ants.

Background for ACS: In nature when real ants are searching for foods, multiple ants are going out in random paths. As the ant is moving, it deposits a chemical substance which is called pheromone on its moving path for guiding other subsequent ants to its path. As the time goes, the pheromone is evaporating. So as the path is shorter as its pheromone concentration remains more time and more other ants are attracted to it. Thus the shortest path is the only one which attracts other ants [13].

More detailed version of the ACS could be found in [17]. As for the ACS based segmentation part, according to their pheromone level and heuristic function value, each pixel is classified as either vessel pixel or background pixel. In this stage, heuristic function value is computed for each pixel with the following equation:

$$\eta^* = \frac{P(v/Vessels)}{P(v/Background)}$$

(8)

Equation above is improved for better segmentation results where P (v/Vessels) and P (v/Background) are the likelihood of feature value v for vessels and background classes respectively [1]. After this process is done, a pheromone map is generated and vessels on this map are segmented with thresholding.

In post-processing step, firstly disjoined pixels are handled. If a pixel is surrounded with at least four neighboring pixels, its value is assigned as 1 and 0 if otherwise. Secondly, regions which have area less than 20 pixels are removed. Finally, a median filter of size 3*3 eliminates all remaining isolated noisy pixels [13].

Proposed method needs to be improved as the accuracy they've achieved is not much competitive against the state-of-the-art methods however, they've achieved quite good sensitivity because of the simplicity of its used features. Their performance achievements are presented in fig. 2.

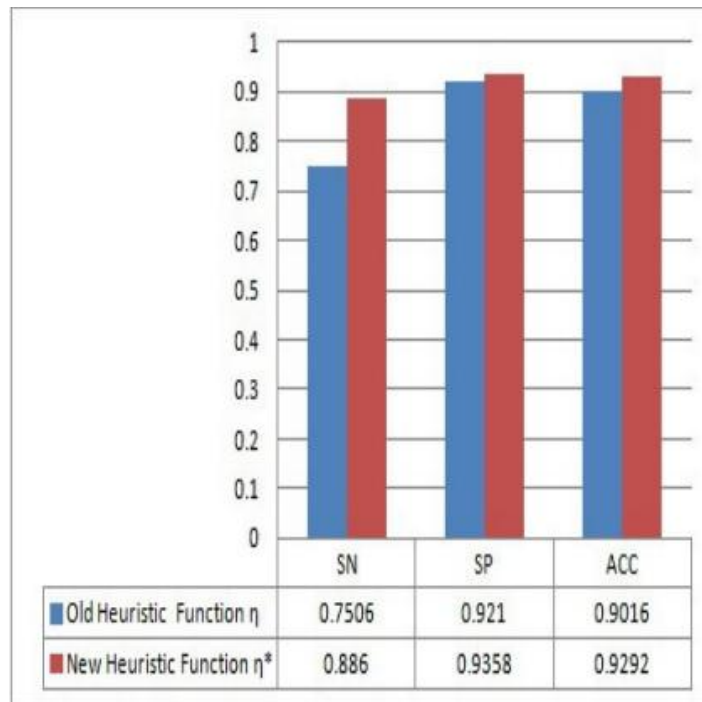|	SN	SP	ACC
Old Heuristic Function η	0.7506	0.921	0.9016
New Heuristic Function η*	0.886	0.9358	0.9292

Figure 2

Database used in these experiments is the STARE [25] database. In the future, experiments should include the database DRIVE [11] and by focusing more on false positives reduction, performance in terms of specificity and accuracy should be improved in order to be competitive against state-of-the-art methods.

3) Rician Denoise Algorithm & Thresholding

In 2016, another study about blood vessel segmentation has been proposed by Kimmy Mehta and Navpreet Kaur from Punjabi University. They obtained background image with morphological operations and performed the segmentation using thresholding method. The working principle of this method is shown in figure 3.
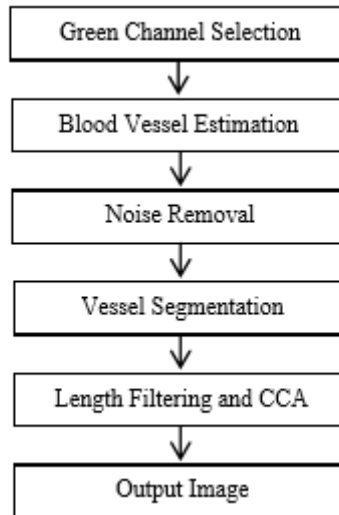

Figure 3 Proposed Segmentation Process

Like the research presented in the previous works, they also used green channel for the detection and segmentation of retinal blood vessels from the retinal image because the green channel is high sensitive to the blood vessels [18]. In other words, it has been considered in existing vessel segmentation studies since it has higher contrast compared to other channels [19-20]. Detection of green channels, using basic morphological processes and thresholding methods, is used for the emergence of vascular structure in RGB retinal images and segmentation of blood vessels.

They wanted to get the original image by removing the background retinal image from the image. The background image is estimated [21] using morphological operations [22]. In this study they've used morphological closing operation to find the background retinal image. Since closing operation suppresses dark details smaller than the structuring element [21]. They tried to produce the background by removing the vessels in the retinal image.

However, because of the still existing noise from original image was a problem, they had to remove even the slightest noise in the image to get the highest quality possible. The image denoising process involves image transformation that can be easily identified by noise, and then is reversed to reduce noise [20]. They've used Rician Denoise algorithm [23], which is a total variation based algorithm [21] that tries to remove noises, to overcome this problem.

The vascular structure of the retinal image is divided using the thresholding method proposed by Phansalkar et al. [24] in 2011. To adapt this method to their problems, they attempted to solve their problems by changing the thresholding scheme globally instead of locally [21]. This is done by changing the size of the local search area according to whole image. Then a calculated threshold is used for the vascular structure and is expressed as:

$$T = mean(f) \left[1 + pe^{-q*mean\,(f)} + k\left(\frac{std(f)}{R} - 1\right) \right]$$

(9)

The parametric values in this method are $k = 0.25$, $p = 2$, $q = 10$ and $R = 0.5$. These values are selected according to the accuracy values by selecting a few combination values. The set with the highest accuracy value obtained from the selected combinations is the last set and theses values are fixed for all datasets.

After these operations, the image of the segmentation process does not give sufficient determination to examine any disease. They did two post-processing for this problem and to improve the performance of this algorithm. First one for removing the spur pixels for final enhancements and second one for removing any region which is not belong to the actual vascular structure. From these, area filtering is an application used to erase the spur pixels that do not belong to the vascular structure. This method is done using the Connected Component Analysis (CCA) technique, in which the image is labeled according to the pixel connections in the different components [23] and these connections are 4 or 8 connectivity. In this study, 8-way connectivity was used.

The performance of the proposed algorithm is evaluated in two databases for automatic segmentation. Databases were DRIVE database [11] and the STARE database [25], which includes half of the number of images inside the DRIVE. The developed method is evaluated with sensitivity (SE), specificity (SP) and accuracy (ACC) metrics and these evaluation methods are calculated with the following formulas.

$$SE = \frac{TP}{TP + FN}$$

$$SP = \frac{TN}{TN + FP}$$

$$ACC = \frac{TP + TN}{TP + FP + FN + TN}$$

(10)

From these formulas, True Positive (TP) represents correctly classified vessel pixels, False Positive (FP) represents non-vessel pixels incorrectly classified as vessel, False Negative (FN) represents vessel pixels incorrectly classified as non-vessel and True Negative (TN) represents correctly classified non-vessel pixels [22].

The average accuracy for the DRIVE database is 94.35%, the average specificity is 98.13% and the sensitivity is 68.15%. The average accuracy for the STARE database is 94.49%, the average specificity is 72.12% and the sensitivity is 97.01%.

This method performed better when compared to previous years' work and gave similar results. This simplicity, robustness, rapid implementation and effectiveness of this algorithm can be suitable method for pre-screening systems for early detection.

4) Image Matting Technique

In 2017, another study related for vessel segmentation has done by Zhun Fan, Jiewei Lu, Wenji Li, Caimin Wei, Han Huang, Xinye Cai and Xinjian Chen. They actually come up with a different technique so called image matting and their proposed method is called hierarchical image matting model. They argued that image matting has never been used to segment blood vessels [26].

Image matting aims to extract the foreground of the image accurately. More specifically, modeling the input image as a linear combination of background and foreground images, producing this equation:

$$I(z) = \alpha z F(z) + (1 - \alpha z)B(z) \quad (11)$$

Where αz value called as the alpha matte indicates it is the opacity of the foreground image, and ranges between 0 and 1. As can be understood from this equation, if αz is forced to be either 0 or 1, the matting problem becomes the segmentation problem because we do not know which pixels belong to the foreground image and which pixels belong to the background image. Proposed method deals with this situation in an efficient way.

It is vital to enhance the image before any process has applied in order to perform segmentation efficiently [2]. They've used two efficient filters to enhance the input image which are Morphologically Reconstructed Filter [27] and the other one is the Isotropic Undecimated Wavelet Filter [28]. Both of these filters extract the green channel image since green channel image provides the best vessel-background contrast and it has much less noise compared to the red and blue channels [29].

They've used argued that creating a user-specified trimap is very time consuming and requires high amount of effort [26] therefore, they've decided to develop another process for generating the trimap automatically. Below figure represents their trimap generation process:
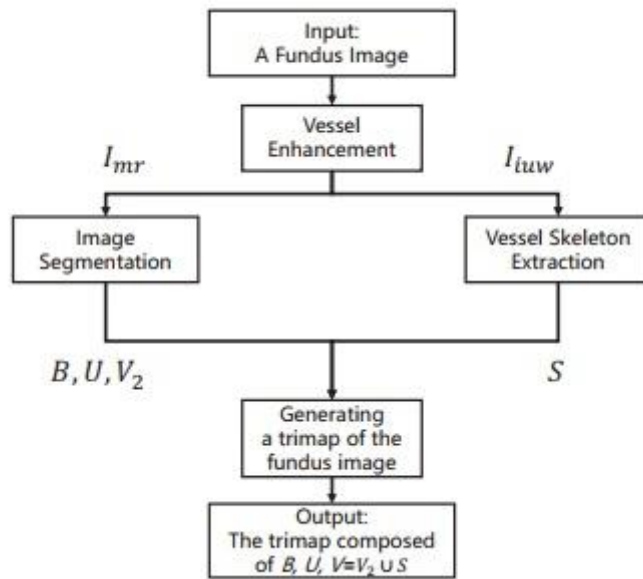

Figure 4

As can be seen in fig 4, process of generating trimap consist of two main steps, image segmentation and vessel skeleton extraction. Image segmentation part deals with the image which was enhanced with the morphologically reconstructed filter whereas the vessel skeleton extraction part deals with the image which was enhanced with the undecimated wavelet filter. At image segmentation part, enhanced image is segmented into three regions which are unknown regions (shown as U in fig 4), background regions (shown as B in fig 4) and preliminary vessel regions (V1). Because of V1 still contains regions with unwanted noise, image has to be denoised, resulting the denoised preliminary vessel regions (shown as V2 in fig 4). At skeleton extraction part, for the purpose of providing more

8

information about vessel skeleton and unknown regions, firstly by applying global thresholding to the enhanced image, binary image T is obtained. Then T is divided into three parts according to the area feature.   Then the regions in T2 with Extent > e2 && V Ratio ≤ r are preserved as T4. Finally extraction [30] process is applied on combined version of T3 and T4 in order to obtain skeleton of blood vessels (shown as S in fig 4). After applying both skeleton extraction and image segmentation parts, trimap is generated with combining background regions, unknown regions and foreground regions which is the union of V2 and S.

For the purpose of handling pixels at the unknown regions, they've implemented a hierarchical image matting model to check if the pixels in the unknown region are background pixel or a vessel pixel. This implementation includes 2 steps. First one is stratifying the unknown pixels. In this step, for each pixel in the unknown region a distance value is obtained. This value is the distance between the unknown region pixel and the nearest vessel pixel. Then, distance values are sorted in ascending order and same distance values are grouped into one hierarchical layer in order to create a hierarchical order set. Needless to say, which is also in ascending order?

Second step is hierarchical update where new labels (V or B) are assigned to each pixel in each hierarchical set member by checking whether it is a background pixel or a vessel pixel. We already have a labeled pixel set consist of background and vessel pixels returned from the trimap generation process. We'll now use those sets for updating our unknown pixels in each hierarchy by calculating their correlations (function definition has given in the paper [26], equation 13) to its neighboring labeled pixels (9x9). After those calculations we chose the pixel with nearest correlation value and give the label of it to the unknown pixel (V or B). This method also has a post-processing method where they remove misclassified vessel regions in order to obtain highest accuracy value possible.

Their experiments show that their model is vastly competitive. Image matting model has been tested with three different databases, DRIVE [11], STARE [25] and CHASE_DB1, which includes 28 fundus images with large variety. Accuracy percentages they measured are %96, %95.7 and %95.1 for DRIVE, STARE and CHASE_DB1 respectively. They achieved fairly low computing time for such accuracy values.

References

1. Roychowdhury, S., Koozekanani, D.D., Parhi, K.K.: Blood vessel segmentation of fundus images by major vessel extraction and sub-image classification. IEEE J. Biomed. Health Inform. 99 (2014). doi:10.1109/JBHI.2014.2335617.

2. M. M. Fraz, P. Remagnino, A. Hoppe, B. Uyyanonvara, A. R. Rudnicka, C. G. Owen, and S. A. Barman, "Blood vessel segmentation methodologies in retinal images–a survey," Computer Methods and Programs In Biomedicine, vol. 108, no. 1, pp. 407–433, 2012.

3. Bhuiyan, A., Nath, B., Chua, J., & Kotagiri, R. (2007). Blood Vessel Segmentation from Color Retinal Images using Unsupervised Texture Classification. *2007 IEEE International Conference on Image Processing*. doi:10.1109/icip.2007.4379880.

4. Tingbiao Chen, Liangzheng Xia, "Digital image processing", Beijing: Posts & Telecommunications Press, 1994.

5. J. C. Dunn (1973): "A Fuzzy Relative of the ISODATA Process and Its Use in Detecting Compact Well-Separated Clusters", *Journal of Cybernetics* 3: 32-57

6. J. C. Bezdek (1981): "Pattern Recognition with Fuzzy Objective Function Algoritms", Plenum Press, New York

7. G. W. Wyszecki and S. W. Stiles, "Color science: Concepts and methods, quantitative data and formulas," New York, Wiley, 1982.

8. J. Geusebroek, R. V. D. Boomgaard, A. W. M. Smeulders, and H. Geerts, "Color invariance," IEEE Transactions on Pattern Analysis and Machine Intelligence, vol. 23(2), pp. 1338–1350, 2001.

9. D. Wu, M. Zhang, and J. Liu, "On the adaptive detection of blood vessels in retinal images," IEEE Transactions on Biomedical Engineering, vol. 53(2), pp. 341– 343, 2006.

10. P. Kruizinga and N. Petkov, "Non linear operator for oriented texture," IEEE Transactions on Image Processing, vol. 8(10), pp. 1395–1407, 1999.

11. Research Section, Digital Retinal Image for Vessel Extraction (DRIVE) Database. Utrecht, the Netherlands, Univ. Med. Center Utrecht, Image Sci. Inst. [Online]. Available: http://www.isi.uu.nl/Research/Databases/DRIVE

12. A. Hoover, V. Kouznetsova, and M. Goldbaum, "Locating blood vessels in retinal images by piece-wise threshold probing of a matched filter response," IEEE Transactions on Medical Imaging, vol. 19(3), pp. 203–210, 2000.

13. Ahmed. H. Asad, A. T. Azar, M. M. M. Fouad and A. E. Hassanien. (2013). An Improved Ant Colony System for Retinal Blood Vessel Segmentation. Computer Science and Information Systems: *Proceedings of the Fedcsis.* (pp. 199-205). Krakow: IEEE.

14. M.K. Hu, "Visual pattern Recognition by Moment Invariants," IRE. Trans. Inform. Theory. , vol. 8, no. 2, 1962.

15. M.A. Hall, "Correlation-based feature selection for discrete and numeric class machine learning," ICML, 2000.

16. M. Dorigo and L.M. Gambardella, "Ant colony system: a cooperative learning approach to the traveling salesman problem," IEEE Trans. Evol. Comput. vol. 1, no. 1, pp. 53–66, 1997.

17. Ahmed. H. Asad, A. T. Azar, and A. E. Hassanien, "Integrated features based on gray-level and Hu moment invariants with ant colony system for retinal blood vessels segmentation," Int. J. Syst. Boil. Biomed. Tech., vol. 1, no. 4, pp. 61-74, 2012.

18. Raja, D. S., Vasuki, S., & Kumar, D. R. (2014). Performance Analysis of Retinal Image Blood Vessel Segmentation. *Advanced Computing: An International Journal, 5*(2/3), 17-23. doi:10.5121/acij.2014.5302

19. Joao V. B. Soares, Jorge J. G. Leandro, Roberto M. Cesar Jr., Herbert F. Jelinek, and Michael J. Cree, "Retinal Vessel Segmentation Using the 2- D Gabor Wavelet and Supervised Classification", IEEE Trans. Med. Imag., 2010.

20. Dalwinder Singh, Dharamveer, Birmohan Singh, "New Morphology based Approach for Blood Vessel Segmentation in Retinal Images,"

21. Mehta K, and Kaur N.: "An Enhanced Segmentation Technique for Blood Vessel in Retinal Images.". International Journal of Computer Applications, vol. 150, no. 6, 2016, pp. 4–5., doi: 10.5120/ijca2016911548.

22. Rosenfeld, A., and Pfaltz, J. L. (1996) „Sequential operations in digital picture processing", Journal of the ACM, Vol. 13 No. 4, pp. 471–494.

23. P. Getreuer, M. Tong, and L. A. Vese. A variational model for the restoration of MR images corrupted by blur and rician noise. In Proc. ISVC, pages 686–698, 2011.

24. Phansalkar, Neerad, Sumit More, Ashish Sabale, and Madhuri Joshi. "Adaptive local thresholding for detection of nuclei in diversity stained cytology images." In Communications and Signal Processing (ICCSP), 2011 International Conference on, pp. 218-220. IEEE, 2011.

25. STARE ProjectWebsite. Clemson, SC, Clemson Univ. [Online]. Available: http://www.ces.clemson.edu/

26. Fan Z., Lu Z., Li W., Wei C., Huang H., Cai X., Chen X.: A Hierarchical Image Matting Model for Blood Vessel Segmentation in Fundus images, 2017.

27. M. M. Fraz, P. Remagnino, A. Hoppe, B. Uyyanonvara, A. R. Rudnicka, C. G. Owen, and S. A. Barman, "An ensemble classification-based approach applied to retinal blood vessel segmentation," IEEE Transactions on Biomedical Engineering, vol. 59, no. 9, pp. 2538–2548, 2012.

28. P. Bankhead, C. N. Scholfield, J. G. McGeown, and T. M. Curtis, "Fast retinal vessel detection and measurement using wavelets and edge location refinement," PloS One, vol. 7, no. 3, p. e32435, 2012.

29. D. Mar´ın, A. Aquino, M. E. Gegundez-Arias, and J. M. Bravo, "A new ´ supervised method for blood vessel segmentation in retinal images by using gray-level and moment invariants-based features," IEEE Transactions on Medical Imaging, vol. 30, no. 1, pp. 146–158, 2011.

30. L. Lam, S.-W. Lee, and C. Y. Suen, "Thinning methodologies-a comprehensive survey," IEEE Transactions on Pattern Analysis and Machine Intelligence, vol. 14, no. 9, pp. 869–885, 1992.